Tropical Journal of Pharmaceutical Research December 2022; 21 (12): 2651-2658
ISSN: 1596-5996 (print); 1596-9827 (electronic)

Available online at http://www.tjpr.org
http://dx.doi.org/10.4314/tjpr.v21i12.21

Original Research Article

A bioinformatics approach to the identification of hub genes of Huo Xin Pill (HXP) for the treatment of acute myocardial infarction

Qiang Yang[1], Juncan Ding[1], Ziyue Luo[1], Pengfei Hu[2]*
[1]The Second Clinical Medical College of Zhejiang Chinese Medical University, [2]Department of Cardiology, The Second Affiliated Hospital of Zhejiang Chinese Medical University, Hangzhou, China

For correspondence:* ***Email:* *20064012@zcmu.edu.cn;* ***Tel:*** *+86-15267037741*

Sent for review: 9 July 2022 *Revised accepted: 27 November 2022*

Abstract

Purpose: *To apply bioinformatics for the identification of potential genes associated with Huo Xin Pill (HXP), a traditional Chinese medicine (TCM) used for the treatment of acute myocardial infarction (AMI).*
Methods: *Mouse AMI expression profile dataset GSE153485 and HXP-treated mouse AMI expression profile dataset GSE147365 were downloaded from GEO database. Then, R software was used to screen differentially-expressed genes in AMI and differentially-expressed genes in HXP-treated AMI. Gene Ontology (GO) enrichment analysis, Kyoto Encyclopedia of Genes and Genomes (KEGG) pathway enrichment analyses, Venn diagrams, and protein-protein interaction (PPI) analysis were carried out on the hub genes linked to the effect of HXP on AMI.*
Results: *Six hub genes were identified. Based on the differential analysis of the sham and AMI groups, GSE153485 and GSE147365 had 840 and 2116 differentially-expressed genes, respectively ($p < 0.05$). The GO and KEGG analyses revealed enrichments in actin filament organization, membrane repolarization, and regulation of the actin cytoskeleton. Differential analysis of the use of HXP on AMI showed that GSE147365 had 380 differentially-expressed genes, comprising 96 up-regulated genes and 284 down-regulated genes ($p < 0.05$). Thirteen potential acting target genes were obtained using a Venn diagram, while 6 key acting genes were obtained via final screening.*
Conclusion: *Six (6) hub genes linked to HXP and AMI have been identified using bioinformatics: Egr2, Tubb2a, Col4a2, Cnn2, Lmna, and Col4a1. This study provides a partial experimental basis for the use of HXP in the treatment of AMI. In addition, it provides new potential targets for the treatment of AMI.*

Keywords: *Huo Xin Pill, Acute myocardial infarction, Bioinformatics, Hub genes, Mechanistic studies*

Tropical Journal of Pharmaceutical Research is indexed by Science Citation Index (SciSearch), Scopus, Web of Science, Chemical Abstracts, Embase, Index Copernicus, EBSCO, African Index Medicus, JournalSeek, Journal Citation Reports/Science Edition, Directory of Open Access Journals (DOAJ), African Journal Online, Bioline International, Open-J-Gate and Pharmacy Abstracts

INTRODUCTION

Acute myocardial infarction (AMI) refers to myocardial necrosis caused by acute and persistent ischemia and hypoxia in the coronary arteries, and it is the most serious type of coronary heart disease. The disease seriously endangers the health of many people worldwide, and it is associated with high morbidity and mortality. Studies have revealed that the

incidence of AMI and its mortality rate are increasing rapidly in China [1]. Although there are significant advances in the development of interventional techniques for AMI, not much progress has been made concerning drugs for the treatment of the disease. Therefore, it is essential to develop new drugs for the treatment of AMI. The pathogenesis of cardiovascular diseases, including AMI, often involves multiple factors, rather than a single factor/pathway.

Therefore, the use of herbal medicines may become a new and promising approach for treating AMI since it has multiple therapeutic targets and multiple therapeutic pathways that work in synergy. Moreover, herbal medicines have attracted extensive worldwide attention as sources of new drugs.

Huo Xin Pill (HXP), as a classical Chinese herbal formula, is a combination of split and combined formulae of *Wu Tou Chi Shi Li Wan* and *Ginseng* and *Phyllanthus Tang*. It contains 10 herbal medicines such as *Ganoderma lucidum*, artificial musk, bear bile, safflower, *in vitro* cultivated cowry, pearl, ginseng, toadstool, epiphyllum, and ice chips [2]. In China, HXP has been clinically proven to manifest pleiotropic effects by protecting the cardiovascular system. These effects comprise improvement of microcirculation, enhancement of coronary flow, improvement of left ventricular beat volume, and enhancement of myocardial contractility, all of which mitigate myocardial ischemia, improve cardiac function and regulate cardiac rhythm [3]. It has been reported that HXP significantly reduced myocardial fibrosis in rats with heart failure by inhibiting the TGF-beta1/Smad2/3 axis, although the specific targets of HXP in AMI treatment are still unclear [4].

With the rapid development of high-throughput gene sequencing technology and bioinformatics, it is now possible to unravel the potential mechanisms underlying the use of Chinese medicine in the treatment of certain diseases. To further understand the mechanism involved in the cardioprotective effects of HXP, this study combines bioinformatics and traditional Chinese medicine to screen and predict the associated potential targets and signaling pathways using Gene Expression Omnibus (GEO), differential gene analysis, enrichment analyses (GO and KEGG) and protein-protein interaction network analysis (PPI).

This study provides not only new evidence for the treatment of AMI with Chinese medicine but also new potential targets for the treatment of AMI.

METHODS

GEO database

The datasets of expression profiles used in this study were obtained from the public database of the GEO National Bioinformatics Institute (https://www.ncbi.nlm.nih.gov/geo) which contains a large number of datasets for gene expression profile arrays and high-throughput sequencing. The GSE153485 dataset containing 10 sham samples and 10 AMI samples from heart tissues was obtained through retrieval using the hub words "myocardial infarction", HXP, and “mouse”. The dataset GSE147365, which was obtained after searching with the hub words, contained 6 sham samples, 6 AMI samples, and 6 HXP samples. All samples were obtained from mouse myocardial tissue.

Data pre-processing and identification of DEGs

The original dataset was obtained from GEO. Samples in the GSE153485 dataset were divided into two groups, i.e., sham and AMI, and differential expression analysis was performed using the Limma package from R (4.1.1), with setting thresholds of $|\log FC| > 0.5$ and $p < 0.05$. Similarly, samples in the GSE147365 dataset were divided into AMI and HXP-treated groups, with differential expression analysis performed using the limma package, set at thresholds of $|\log FC| > 0.5$ and $p < 0.05$. The results of differential expression analysis were visualized and analyzed using the ggplot2 package and heatmap package to create volcano and heat maps.

Differential gene enrichment analysis

The cluster profiler package, ggplot2 package, and GOplot package of R were used for enrichment analysis and visualization of differently-expressed genes.

Identification of hub genes

The STRING database was used to construct PPI networks for DEGs. The numbers of network nodes were plotted, and nodes with node number > 5 were screened as hub-acting targets.

Expressions of hub genes

The expressions of hub targets in the sham, AMI, and HXP were analyzed and box plots of expression differences were drawn.

Statistical analysis

The data were pre-processed and analyzed using SPSS 22.0 and R software. The pre-processing involved sample data merging, ID transformation, and elimination of duplicates. Graphs were constructed using R software, GraphPad Prism, and online plotting tools. Values of $p < 0.05$ were assumed indicative of statistically significant differences among groups.

RESULTS

DEGs for sham and AMI

Expression data of GSE153485 and GSE147365 were analyzed for differences based on sham and AMI groups. A total of 840 differential genes were obtained for GSE153485, comprising 603 up-regulated and 237 down-regulated genes. Volcano and heat maps were plotted for the differential results, as shown in Figures 1 A and C.

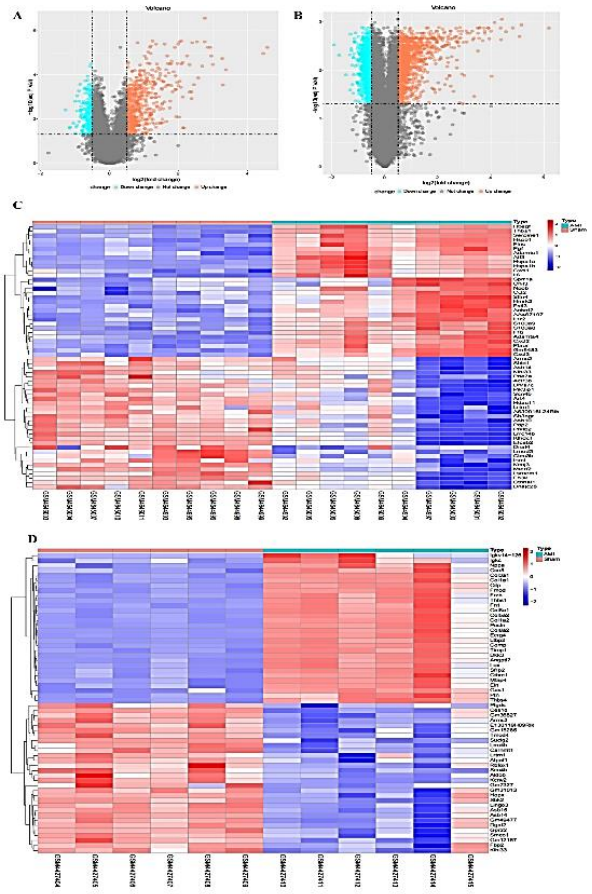

Figure 1: Differential gene analysis of sham relative to AMI in mice. (A) GSE153485 dataset volcano plot, (B) GSE147365 dataset volcano plot, (C) GSE153485 dataset heat map, (D) GSE147365 dataset heat map. (|log FC| > 0.5, $P < 0.05$)

In contrast, 2116 differentially-expressed genes were obtained for GSE147365, and these comprised 1197 up-regulated and 919 down-regulated genes. Volcano and heat maps were plotted for the differential results, as depicted in Figures 1 B and D.

GO and KEGG enrichment analysis of sham relative to AMI

The results of the analysis of GSE147365 and GSE153485 datasets were plotted as Venn diagrams, and the genes simultaneously up-regulated or down-regulated were used as differential genes of AMI, relative to sham. As shown in Figure 2 A, 175 differential genes were up-regulated, while 116 genes were down-regulated. Then GO and KEGG enrichment analyses were performed on the up-regulated genes. The GO analysis revealed that the up-regulated genes were significantly enriched in biological processes (BPs) such as actin filament organization, cell-substrate adhesion, and regulation of cell-substrate adhesion, actin cytoskeleton. Concerning cellular components (CCs), the up-regulated genes were significantly enriched in actin filament bundle and stress fiber, while the enriched molecular functions (MFs) were actin binding, actin filament binding, and cell adhesion molecule binding.

KEGG analysis showed that these up-regulated genes were enriched in the regulation of actin cytoskeleton, focal adhesion, and proteoglycans in cancers (Figure 2 B). Moreover, GO and KEGG enrichment analyses were performed on the down-regulated genes. The GO analysis showed that the down-regulated genes were significantly enriched in membrane repolarization, cardiac muscle cell action potential, cardiac muscle cell membrane repolarization, regulation of membrane repolarization and other BPs, T-tubule, sarcoplasmic reticulum, sarcoplasm, sarcolemma, and other CCs, potassium channel activity, flavin adenine dinucleotide binding, FAD binding, and voltage-gated potassium channel activity and other MFs. In contrast, KEGG analysis did reveal significant enrichment. These results are shown in Figure 2 C.

Differential enrichment analysis of HXP in relation to AMI

Differential analysis of the expression data from the GSE147365 dataset in relation to HXP and AMI showed 380 differentially-expressed genes, comprising 96 up-regulated genes and 284 down-regulated genes. Volcano and heat maps of the differentially-expressed genes were plotted

(Figures 3 A and B), and GO and KEGG enrichment analyses were performed. The GO analysis revealed that the differentially-expressed genes were significantly enriched in the cellular response to stimulus from transforming growth factor beta, transmembrane receptor protein serine/threonine kinase signaling pathway, and other BPs while KEGG analysis showed that they were enriched in non-alcoholic fatty liver disease, amphetamine addiction, and circadian rhythm (Figures 3 C and D; Supplement Table 1).

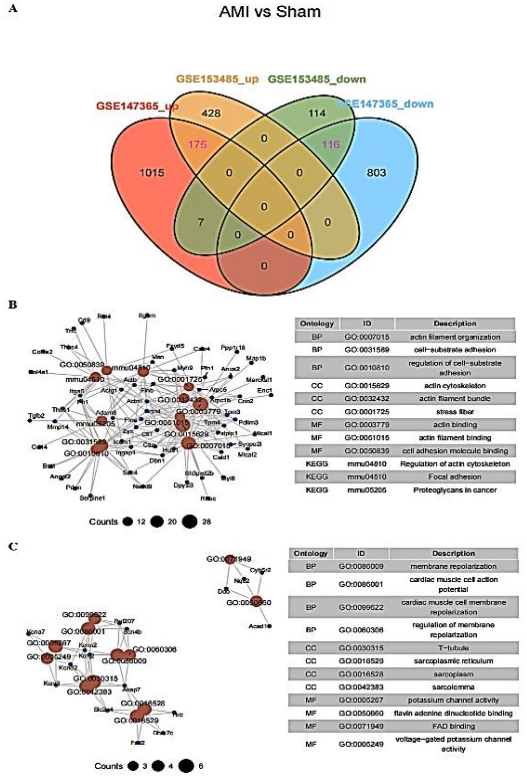

Figure 2: Screening and analysis of differential genes in AMI vs Sham. (A) Venn diagram of the GSE147365 dataset and GSE153485 dataset, with a total of 175 differential genes up-regulated and 116 differential genes down-regulated. (B) GO and KEGG enrichment analysis of AMI vs Sham up-regulated differential genes; (C) GO and KEGG enrichment analysis of AMI vs Sham down-regulated differential genes

HXP for AMI hub gene screening

To identify the hub genes involved in the effect of HXP on AMI, differentially-expressed genes with respect to HXP vs AMI and AMI vs sham were taken as intersections and were screened for up-regulation in HXP vs AMI, and down-regulation in AMI vs sham, or down-regulation in HXP vs AMI and up-regulation in AMI vs sham. These screenings resulted in the identification of 13 potential target genes (Figure 4 A). Through GO analysis, it was found that the 13 potential target genes were significantly enriched in collagen-activated tyrosine kinase receptor signaling pathway, collagen-activated signaling pathway, skeletal muscle cell differentiation, and other biological processes (complex of collagen trimers, extracellular matrix components, collagen trimers), and other cellular components, as well as extracellular matrix structural constituent conferring tensile strength, activin binding, and other molecular functions (Figure 4 B). Moreover, KEGG analysis revealed that these target genes were enriched in ECM-receptor interaction, small cell lung cancer, and the AGE-RAGE signaling pathway in diabetic complications (Figure 4 C).

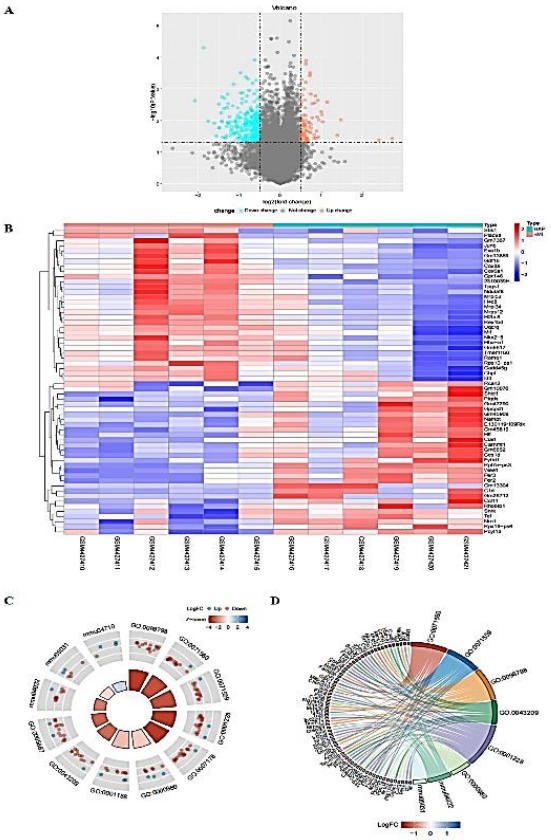

Figure 3: Differential gene analysis of HXP relative to AMI, showing 380 differential genes, comprising 96 up-regulated genes and 284 down-regulated genes. (A) Volcano plot, (B) Heat map, (C) Circle plot of GO and KEGG enrichment analysis, (D) Chord plot of GO and KEGG enrichment analysis. (|log FC| > 0.5, p < 0.05)

PPI network of hub genes

In this study, PPI networks of the 13 potential targets were constructed for further screening of related hub genes (Figure 5 A). Based on the results of PPI networks, the numbers of connected nodes for each potential target were plotted (Figure 5 B), and genes with nodes greater than 5 were selected as hub-acting

targets of HXP. Finally, 6 hub-acting genes were obtained: Egr2, Tubb2a, Col4a2, Cnn2, Lmna, and Col4a1.

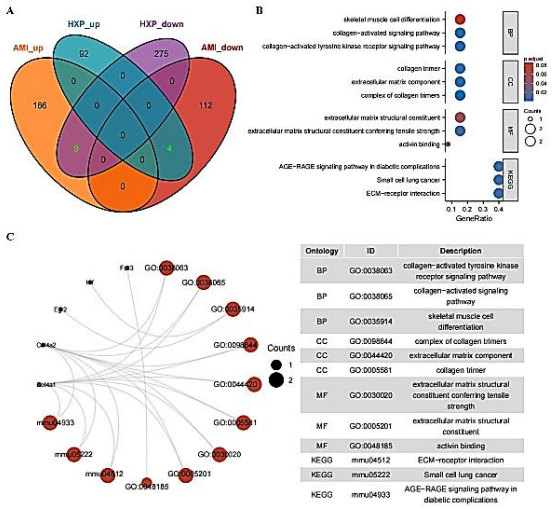

Figure 4: Differential gene screening and analysis of HXP for AMI. (A) Differentially-expressed genes with respect to HXP vs AMI and AMI vs sham were taken as intersections, (B) Bubble diagram for GO and KEGG enrichment analysis of differential genes, (C) Bubble diagram for HXP for AMI differential gene GO and KEGG enrichment analysis network plots

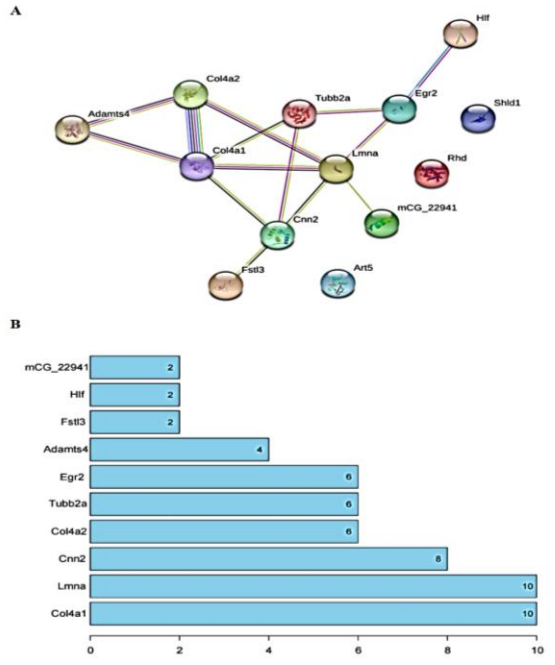

Figure 5: Screening of hub-acting targets for HXP. (A) PPI network construction for 13 hub genes, (B) Number of nodes connected to hub genes for PPI network results

Expressions of hub genes across groups

The expressions of hub target genes in sham, AMI, and HXP-treated groups were analyzed, and expression box line plots were drawn (Figure 6). As can be seen from the graph, the expressions of Egr2, Tubb2a, Col4a2, Cnn2, Lmna, and Col4a1 did not significantly differ, relative to HXP-treated and sham ($p > 0.05$), but they differed significantly between AMI and sham and between AMI and HXP-treated groups ($p < 0.05$). All the hub genes were highly expressed in AMI.

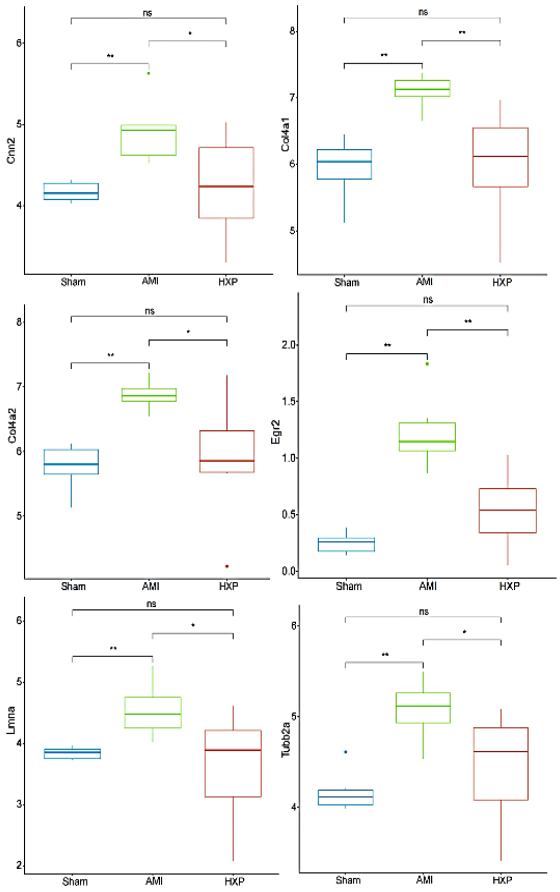

Figure 6: Box plot of expression of 6 hub target genes in sham, AMI, and HXP. $P > 0.05$ (ns), $*p < 0.05$, $**p < 0.001$

DISCUSSION

The mortality rate of AMI has been significantly reduced, due to advancements in interventional techniques and drug therapy, although, it is still high when compared to other diseases. Therefore, new therapeutic targets and new drugs are of great importance for the reduction of AMI mortality. Since the advent of the COVID-19 pandemic, TCM has attracted increased attention from countries around the world due to its high therapeutic efficacy.

Similarly, herbal formulas have played significant roles in the treatment of cardiovascular diseases [5]. It has been reported that GAO-ZI-YAO is

used for treating spontaneous hypertension in elderly rats through a mechanism involving an increase in serum NO levels and inhibition of serum Angiotensin II levels. Compared with conventional treatment involving atrial fibrillation, the addition of heart-stabilizing granules improved left ventricular ejection fraction and reduced BNP levels in patients with chronic heart failure combined with atrial fibrillation, thereby improving their cardiac functions [6]. Raw pulse is a TCM, which has long been used as a complementary treatment for Chinese patients with chronic heart failure. In one multi-center cohort study of 1211 patients with chronic heart failure, raw pulse was shown to improve cardiac function in patients with CHF, and it had a good safety profile [7].

Unfortunately, the targets of many Chinese herbal medicines for related diseases are still unclear. This constitutes an obstacle to the further development of Chinese medicine. Therefore, there is a crucial need to study the therapeutic targets of Chinese herbal formulas. In this study, 175 up-regulated and 116 down-regulated differentially-expressed genes were screened for AMI. Bioinformatics analyses of GSE153485 and GSE147365 datasets revealed 96 up-regulated and 284 down-regulated differential genes after HXP treatment of AMI. To identify the hub genes in the treatment of AMI with HXP as a TCM formula, Venn diagrams were used to identify genes that were up-regulated relative to those down-regulated with HXP in AMI, and a total of 13 genes were screened out. To gain a deeper understanding of the biological functions of the 13 hub genes, GO and KEGG enrichment analyses were performed. The GO analysis indicated that these hub genes were enriched in collagen-activated tyrosine kinase receptor signaling pathway, and other BPs, while KEGG analysis revealed that they were enriched in ECM-receptor interaction and other pathways. Finally, a PPI network of the 13 hub genes was constructed, through which 6 hub genes (Egr2, Tubb2a, Col4a2, Cnn2, Lmna, and Col4a1) were selected as potential hub genes in the HXP for AMI. All 6 hub genes were highly expressed in AMI myocardial tissues.

Early growth response protein 2 (Egr2), a gene that encodes the Egr2 transcription factor, is involved in the regulation of cell growth, differentiation, and apoptosis, regulation of the proliferation and differentiation of T/B cells, as well as participation in the immune response. However, recent studies have found that silencing EGR2 in AMI mice reduced cardiomyocyte apoptosis and increased ATP content, thereby reducing the impairment of cardiac function after AMI [8]. This is consistent with the finding that EGR2 is highly expressed in AMI mice, revealing that high expression of EGR2 may be one of the pathways involved in cardiac injuries after AMI.

Tubb2a is the gene that encodes 2A-type-tubulin (TUBB2A), a major component of microtubule structure that plays a central role in maintaining cellular morphology and important movements, for example, mitochondrial migration. A study has revealed that microtubule damage leads to mitochondrial lesions in cardiomyocytes [9]. Indeed, cardiomyocyte mitochondria are often considered to be the hub organelle for cell survival and cell death after AMI [10]. Therefore, TUBB2A may be one of the potential therapeutic targets in AMI.

The genes *Col4a1* and *Col4a2* (also known as canstatin) encode type IV collagen subunits which are major structural components of the basement membrane. Recently, it was found that downregulation of Col4a1 enhanced the proliferation, migration, invasion, and angiogenesis of cardiac microvascular endothelial cells (CMECs) in rat myocardial tissues after ischemic injury, thereby protecting the myocardium after AMI [11]. Cardiomyocytes are encapsulated by the basement membrane. Canstatin modulates the activities of L-type calcium channels through which calcium ions enter the cells, and these channels are essential for normal cardiomyocyte contraction [12]. Furthermore, since canstatin inhibits blood hypoxia-induced apoptosis in H9c2 cardiomyoblasts, canstatin may be effective in the treatment of AMI [13].

The gene *Cnn2* encodes for calmodulin isoform 2. The encoded calmodulin isoform 2 is an actin-binding protein. A study has shown that the knockdown of Cnn2 attenuated myofibroblast differentiation, thereby slowing downs the development of calcific aortic valve disease in ApoE -/- mice [14]. However, the relationship among Cnn2, cardiomyocytes, and AMI has not yet been elucidated. Consequently, there is a need for more studies in this area of AMI research.

Encoded by the *Lmna* gene, the Lamin A protein is a major nuclear protein component in higher postnatal animals, including humans. Mutations in the Lmna gene may lead to the premature aging syndrome, a condition in which patients are highly susceptible to death at the age range of 10 - 20 due to AMI-related complications caused by atherosclerosis [15]. In a study, Lmna expression was elevated in the myocardial tissue

of pigs after AMI [16]. This is consistent with the results reported in the present study. Although the role of Lmna in the pathophysiology of AMI is still unclear, Lmna may be of value in the diagnosis of AMI.

There are many shortcomings in the present study. Firstly, only the sequencing results from other research were analyzed. The results were not validated at the clinical or experimental animal or cellular level. Secondly, the data set selected had a small sample size which may lead to less accurate conclusions. Finally, although some core gene targets were identified, their interrelationships and their roles in the pathophysiological processes involved in AMI were not fully elucidated. To this end, further clinical and basic research is necessary for the identification of the potential HXP-related targets for AMI.

CONCLUSION

This study involves comprehensive analyses of GEO datasets (GSE153485 and GSE147365) using bioinformatics. Six potential hub genes (Egr2, Tubb2a, Col4a2, Cnn2, Lmna, and Col4a1) have been identified for the treatment of AMI using HXP and they are generally highly expressed in the tissues of AMI mice. These results provide a partial scientific basis for the use of HXP in the treatment of AMI, as well as provide new targets for the treatment of AMI.

DECLARATIONS

Acknowledgements

The authors are grateful to all the participants for their contributions to this research article. This study was supported by the Zhejiang Medicine and Health Science and Technology Plan Project (Grant no. 2020KY205) and the Zhejiang TCM Science and Technology Planning Project (Grant no. 2022ZA082).

Funding

None provided.

Ethical approval

None provided.

Availability of data and materials

The datasets used and/or analyzed during the current study are available from the corresponding author on reasonable request.

Conflict of Interest

No conflict of interest associated with this work.

Contribution of Authors

The authors declare that this work was done by the authors named in this article and all liabilities pertaining to claims relating to the content of this article will be borne by them.

REFERENCES

1. *Zhao D, Liu J, Wang M, Zhang X, Zhou M. Epidemiology of cardiovascular disease in China: current features and implications. Nat Rev Cardiol 2019; 16: 203-212.*
2. *He J, Wo D, Ma E, Wang Q, Chen J, Peng J. Network pharmacology-based analysis in determining the mechanisms of Huoxin pill in protecting against myocardial infarction. Pharm Biol 2021; 59: 1191-1202.*
3. *Wang Q, Ma E, Wo D, Chen J, He J, Peng J. Huoxin pill prevents acute myocardial ischaemia injury via inhibition of Wnt/β-catenin signaling. J Cell Molecul Med 2021; 25: 11053-11062.*
4. *Peng M-Z, Yang M-L, Shen AL, Zhou X-L, Lu Y, Li Q. Huoxin Pill Attenuates Cardiac Fibrosis by Suppressing TGF-β1/Smad2/3 Pathway in Isoproterenol-Induced Heart Failure Rats. Chin J Integr Med 2021; 27: 424-431.*
5. *Gao L, Cao M, Li J-Q, Qin X-M, Fang J. Traditional Chinese Medicine Network Pharmacology in Cardiovascular Precision Medicine. Curr Pharm Des 2021; 27: 2925-2933.*
6. *Shi S, Chu Y, Jia Q, Hu Y. Comparative efficacy and safety of wenxin granule combined with antiarrhythmic drugs for atrial fibrillation: A protocol for a systematic review and network meta-analysis. Medicine (Baltimore) 2021; 100: e24434.*
7. *Guan H, Dai G-H, Gao W-L, Zhang T, Sun C, Ren L-L. Effect of Shenmai Injection on Long-Term Prognosis of Patients with Chronic Heart Failure: A Multicenter, Large Sample Capacity, Long-Term Follow-Up Retrospective Cohort Study. Chin J Integr Med 2022; 28: 312-318.*
8. *Cao X, Ma Q, Wang B, Qian Q, Liu N, Liu T. Silencing long non-coding RNA MIAT ameliorates myocardial*

dysfunction induced by myocardial infarction MIAT/miR-10a-5p/EGR2 axis. Aging 2021; 13: 11188-11206.

9. *Craddock TJA, St George M, Freedman H, Barakat KH, Damaraju S, Hameroff S. Computational predictions of volatile anesthetic interactions with the microtubule cytoskeleton: implications for side effects of general anesthesia. PLoS One 2012; 7: e37251.*
10. *Ramachandra CJA, Hernandez-Resendiz S, Crespo-Avilan GE, Lin Y-H, Hausenloy DJ. Mitochondria in acute myocardial infarction and cardioprotection. EBioMed 2020; 57: 102884.*
11. *Yang M, Liu X, Jiang M, Li J, Tang Y, Zhou L. miR-543 in human mesenchymal stem cell-derived exosomes promotes cardiac microvascular endothelial cell angiogenesis after myocardial infarction through COL4A1. IUBMB Life 2021; 73: 927-940.*
12. *Imoto K, Hirakawa M, Okada M, Yamawaki H. Canstatin modulates L-type calcium channel activity in rat ventricular cardiomyocytes. Biochem Biophys Res Commun 2018; 499: 954-959.*
13. *Kanazawa H, Imoto K, Okada M, Yamawaki H. Canstatin inhibits hypoxia-induced apoptosis through activation of integrin/focal adhesion kinase/Akt signaling pathway in H9c2 cardiomyoblasts. PLoS One 2017; 12: e0173051.*
14. *Plazyo O, Liu R, Moazzem Hossain M, Jin JP. Deletion of calponin 2 attenuates the development of calcific aortic valve disease in ApoE mice. J Molecular Cell Cardiol 2018; 121: 233-241.*
15. *Piekarowicz K, Machowska M, Dzianisava V, Rzepecki R. Hutchinson-Gilford progeria syndrome-current status and prospects for gene therapy treatment. Cells 2019; 8.*
16. *Prat-Vidal C, Gálvez-Montón C, Nonell L, Puigdecanet E, Astier L, Solé F. Identification of temporal and region-specific myocardial gene expression patterns in response to infarction in swine. PLoS One 2013; 8: e54785.*